Neutrinoless double-β decay matrix elements in large shell-model spaces with the generator-coordinate method

C. F. Jiao, J. Engel, and J. D. Holt

Phys. Rev. C **96**, 054310 — Published 13 November 2017

DOI: 10.1103/PhysRevC.96.054310

Neutrinoless double-beta decay matrix elements in large shell-model spaces with the generator-coordinate method

C.F. Jiao,[1,2] J. Engel,[1,*] and J.D. Holt[3,†]

[1] *Department of Physics and Astronomy, University of North Carolina, Chapel Hill, North Carolina, 27599-3255, USA*
[2] *Department of Physics, Central Michigan University, Mount Pleasant, Michigan, 48859, USA*
[3] *TRIUMF, 4004 Wesbrook Mall, Vancouver, BC V6T 2A3, Canada*

(Dated: September 12, 2017)

We use the generator-coordinate method with realistic shell-model interactions to closely approximate full shell-model calculations of the matrix elements for the neutrinoless double-beta decay of ^{48}Ca, ^{76}Ge, and ^{82}Se. We work in one major shell for the first isotope, in the $f_{5/2}pg_{9/2}$ space for the second and third, and finally in two major shells for all three. Our coordinates include not only the usual axial deformation parameter β, but also the triaxiality angle γ and neutron-proton pairing amplitudes. In the smaller model spaces our matrix elements agree well with those of full shell-model diagonalization, suggesting that our Hamiltonian-based GCM captures most of the important valence-space correlations. In two major shells, where exact diagonalization is not currently possible, our matrix elements are only slightly different from those in a single shell.

PACS numbers: 21.10.-k, 21.60.-n, 27.40.+z, 27.50.+e

I. INTRODUCTION

Experiments to measure the rate of neutrinoless double-beta ($0\nu\beta\beta$) decay are increasing in number and scale [1], in part because they offer the only real hope of determining whether neutrinos are Majorana particles. The rate of decay, however, depends on nuclear matrix elements that must be accurately calculated to allow experimentalists to plan efficiently and interpret results. At present, the predictions of various nuclear models for the matrix elements differ by factors of up to three [2, 3], and it is not possible to estimate the theoretical uncertainty in any of them. Improving the accuracy of matrix-element calculations has become an important goal for the nuclear-structure community.

The methods used to calculate the matrix elements include the shell model [4–6], the interacting boson model (IBM) [7], the quasiparticle random phase approximation (QRPA) [8–10], and the generator coordinate method (GCM) [11–14]. Both the QRPA and the GCM have been used in conjunction with energy density functional (EDF) theory [8, 12, 13]. These methods, which allow large single-particle spaces (and thus allow unrestricted collective deformation and pairing) but do not contain all kinds of correlations, yield matrix elements that are usually larger than those of the shell model, which employs only a few single-particle levels but allows arbitrarily complex correlations within them. Recent work to compare the shell-model with the GCM [15] suggests that the extra valence-space correlations, particularly those due to isoscalar pairing [16], are responsible for much of the difference in the predictions of the two methods.

In an attempt to include all relevant physics, Ref. [14] proposed combining the virtues of the large-single-particle-space methods with those of the shell model by using the neutron-proton pairing amplitudes as generator coordinates in the GCM approach, within spaces of two or more major shells. Though promising, the results in that paper were obtained with the restriction (as in prior GCM work on $0\nu\beta\beta$ decay [11–13]) that deformation be axially symmetric and with a simple pairing-plus-quadrupole interaction. Here we include a measure of triaxial deformation parameter as a generator coordinate and work with genuine shell-model interactions. We use a one-shell calculation to compare our results, obtained with carefully fit and widely used interactions [6], to those of exact diagonalization with the same interactions. Having verified the accuracy of our approach, we move on to a two-shell spaces, in which exact diagonalization is not currently possible. Because no careful Hamiltonian tuning has yet been done for the $fp-sdg$ model space appropriate for $A \approx 80$, we use the perturbation-theoretic methods discussed in Ref. [17] to derive an interaction. Our results are the first for ^{76}Ge and ^{82}Se of a realistic shell-model-like calculation in more than one shell, and the first exploration of the effects of triaxiality on $\beta\beta$ decay. Recent experiments indicate that the deformation of ^{76}Ge is indeed triaxial [18].

This paper is organized as follows: Section II presents a brief overview of the $0\nu\beta\beta$ matrix elements and of the GCM with a Hamiltonian. Section III contains results in a single shell, which we use to test our approach by comparing with exact diagonalization. Section IV, which presents $0\nu\beta\beta$ matrix elements in two shells, is the heart of the paper. Section V contains a preview of future work and a summary.

* Email: engelj@physics.unc.edu
† Email: jholt@triumf.ca

II. MATRIX ELEMENTS AND METHODS

In the closure approximation, the quantity we need is the matrix element of a two-body operator between the ground states of the initial and final nuclei. If the decay is produced by the exchange of a light-Majorana neutrino with the usual left-handed currents, we can write the nuclear matrix element as [19, 20]

$$M^{0\nu} = M^{0\nu}_{\rm GT} - \frac{g_V^2}{g_A^2} M^{0\nu}_{\rm F} + M^{0\nu}_T \tag{1}$$
$$= \frac{2R}{\pi g_A^2} \int_0^\infty q\, dq\, \langle F| \sum_{a,b} \frac{j_0(qr_{ab})\left[h_{\rm GT}(q)\vec{\sigma}_a\cdot\vec{\sigma}_b + h_{\rm F}(q)\right] + j_2(qr_{ab})h_T(q)\left[3\sigma_1\cdot\vec{r}_{ab}\sigma_2\cdot\vec{r}_{ab} - \sigma_1\cdot\sigma_2\right]}{q + \overline{E} - (E_I + E_F)/2} \tau_a^+\tau_b^+ |I\rangle \ ,$$

where GT, F, and T refer to the Gamow-Teller, Fermi, and tensor parts of the matrix element. The vector and axial coupling constants are given by $g_V = 1$ and $g_A \approx 1.27$, $|I\rangle$ and $|F\rangle$ are the ground-states of the initial and final nuclei, r_{ab} is the distance between nucleons a and b, j_0 and j_2 are the usual spherical Bessel functions, $\bar{E}$ is an average excitation energy (to which the matrix element is not sensitive), and the nuclear radius $R = 1.2A^{1/3}$ fm makes the matrix element dimensionless. The functions $h_{\rm F}(q)$, $h_{\rm GT}(q)$, and $h_{\rm T}(q)$ contain nucleon form factors and forbidden corrections to the weak current. We modify our wave functions at short distances with the "Argonne" correlation function [21]. A detailed presentation of the form of the matrix element can be found in Ref. [20].

The crucial ingredients in Eq. (1) are the initial and final ground states $|I\rangle$ and $|F\rangle$. To obtain them, we use a shell-model effective Hamiltonian $H_{\rm eff}$ in a valence space whose size we are free to choose. The first step in the GCM procedure is to generate a set of reference quasiparticle vacuua $|\varphi(q_1, q_2, \ldots)\rangle$ that provide the minimum energy such states can have while constrained to also have expectation values $q_i = \langle \mathcal{O}_i \rangle$ for a set of collective operators $\mathcal{O}_i$. Here we take the operators $\mathcal{O}_i$ to be:

$$\begin{aligned} \mathcal{O}_1 &= Q_{20}\,, & \mathcal{O}_2 &= Q_{22}\,, \\ \mathcal{O}_3 &= \frac{1}{2}(P_0 + P_0^\dagger)\,, & \mathcal{O}_4 &= \frac{1}{2}(S_0 + S_0^\dagger)\,, \end{aligned} \tag{2}$$

where

$$\begin{aligned} Q_{2M} &= \sum_a r_a^2 Y_a^{2M}\,, \\ P_0^\dagger &= \frac{1}{\sqrt{2}} \sum_l \sqrt{2l+1}\,[c_l^\dagger c_l^\dagger]^{L=0,J=1,T=0}_{000}\,, \\ S_0^\dagger &= \frac{1}{\sqrt{2}} \sum_l \sqrt{2l+1}\,[c_l^\dagger c_l^\dagger]^{L=0,J=0,T=1}_{000}\,, \end{aligned} \tag{3}$$

with M labeling the angular-momentum z-projection and a labeling nucleons, and the brackets signifying the coupling of orbital angular momentum, spin, and isospin to various values, each of which has z-projection zero. The operator $c_l^\dagger$ creates a particle in the single-particle level with orbital angular momentum l. The operator $P_0^\dagger$ creates a correlated isoscalar pair, and the operator $S_0^\dagger$ a correlated isovector neutron-proton pair. We actually only constrain one of the two pair amplitudes at a time: the isoscalar amplitude when computing $M^{0\nu}_{GT}$ (and $M^{0\nu}_T$, which is small) and the isovector amplitude when computing $M^{0\nu}_F$. The usual deformation parameters β and γ are related to $q_1 \equiv \langle Q_{20}\rangle$ and $q_2 \equiv \langle Q_{22}\rangle$ by $\beta = (\chi b^2/\omega_0)\sqrt{q_1^2 + 2q_2^2}$ (with b the oscillator length, given by $2R/\sqrt{5}\,(3A/2)^{-1/6}$, $\omega_0 = 41.2A^{-1/3}$, $\chi = 0.4$) and $\gamma = \tan^{-1}(\sqrt{2}q_2/q_1)$.

To efficiently include the effect of neutron-proton pairing, we start, as in Ref. [14], from a Bogoliubov transformation that mixes neutrons and protons, i.e. from quasiparticle operators of the (schematic) form

$$\alpha^\dagger \sim u_p c_p^\dagger + v_p c_p + u_n c_n^\dagger + v_n c_n. \tag{4}$$

In the full equations single-particle states are summed over, so that each of the coefficients u and v are replaced by matrices, as described in Ref. [22]. We then solve constrained Hartree-Fock-Bogoliubov (HFB) equations, minimizing expectation values of the form

$$\begin{aligned} \langle H' \rangle = \langle H_{\rm eff}\rangle &- \lambda_Z\left(\langle N_Z\rangle - Z\right) - \lambda_N\left(\langle N_N\rangle - N\right) \\ &- \sum_i \lambda_i\left(\langle \mathcal{O}_i\rangle - q_i\right)\,, \end{aligned} \tag{5}$$

where the N_Z and N_N are the proton and neutron number operators, λ_Z and λ_N are corresponding Lagrange multipliers, the sum over i includes up to three of the 4 $\mathcal{O}_i$ in Eq. (2), and the other λ_i are Lagrange multipliers to constrain the expectation values of those operators to q_i. We solve these equations many times, constraining each time to a different point on a mesh in the space of q_i.

Having obtained a set of HFB vacua with various amounts of axial deformation, triaxial deformation, and isoscalar/isovector pairing, we construct the GCM state by superposing projected HFB vacua:

$$|\Psi^J_{NZ\sigma}\rangle = \sum_{K,q} f^{JK}_{q\sigma}\, |JMK; NZ; q\rangle\ , \tag{6}$$

where $|JMK;NZ;q\rangle \equiv \hat{P}^J_{MK}\hat{P}^N\hat{P}^Z|\varphi(q)\rangle$ and q is short for the set of all q_i. Here, the $\hat{P}$'s are projection operators onto states with well-defined angular momentum J and z-component M, neutron number N, and proton number Z [23]. The weight functions $f^{JK}_{q\sigma}$, where σ enumerates states with the same quantum numbers, follow from the Hill-Wheeler equations [23]

$$\sum_{K',q'}\left\{\mathcal{H}^J_{KK'}(q;q') - E^J_\sigma \mathcal{N}^J_{KK'}(q;q')\right\} f^{JK'}_{q'\sigma} = 0, \quad (7)$$

where the Hamiltonian kernel $\mathcal{H}^J_{KK'}(q;q')$ and the norm kernel $\mathcal{N}^J_{KK'}(q;q')$ are given by

$$\begin{aligned}\mathcal{H}^J_{KK'}(q;q') &= \langle\varphi(q)|\, H_{\rm eff}\hat{P}^J_{KK'}\hat{P}^N\hat{P}^Z\,|\varphi(q')\rangle\ ,\\ \mathcal{N}^J_{KK'}(q;q') &= \langle\varphi(q)|\,\hat{P}^J_{KK'}\hat{P}^N\hat{P}^Z\,|\varphi(q')\rangle\ .\end{aligned} \quad (8)$$

To solve Eq. (7), we first diagonalize the norm kernel $\mathcal{N}$ and then use the nonzero eigenvalues and corresponding eigenvectors to construct a set of "natural states." Finally, we diagonalize the Hamiltonian in the space of these natural states to obtain the GCM states $|\Psi^J_{NZ\sigma}\rangle$ (for details, see Refs. [24, 25]). We carry out this entire procedure in both the initial and final nucleus, using the lowest $J = 0$ states in each as the ground states between which we sandwich the $0\nu\beta\beta$ operator to obtain the matrix element $M^{0\nu}$ from Eq. (1).

III. TESTS IN A SINGLE SHELL

Before undertaking a two-major-shell calculation, we need to test our GCM with a realistic interaction in a model space small enough to allow exact diagonalization. We begin by performing GCM calculations in the pf-shell, comprising the $0f_{7/2}$, $0f_{5/2}$, $1p_{3/2}$, and $1p_{1/2}$ orbits. Using use the KB3G interaction [26], which accounts successfully for the spectroscopy, electromagnetic and Gamow-Teller transitions, and deformation of pf-shell nuclei [27], we compute the $0\nu\beta\beta$ matrix elements of ^{48}Ca, ^{54}Ti, and ^{54}Cr. Although the last two nuclei are not candidates for an experiment, they offer opportunities to test the GCM. Because these nuclei show no evidence of triaxial deformation, we need only use the axial quadrupole moment $q_1 \equiv \langle Q_{20}\rangle$ and isoscalar pairing amplitude $\phi \equiv q_3 = 1/2\,\langle P_0 + P_0^\dagger\rangle$ as generator coordinates for the computation of $M^{0\nu}_{GT}$.

Figure 1 shows the GT matrix elements that result from this procedure, alongside those coming from exact diagonalization. To highlight the effects of isoscalar pairing in the GCM, we present the results of two separate GCM calculations. In the first, as in Ref. [16], we set all the two-body matrix elements of the Hamiltonian with angular momentum $J = 1$ and isospin $T = 0$ to zero, because those are the ones through which isoscalar pairing acts. The resulting GT matrix elements overestimate the exact one substantially. In the second calculation, we use the full KB3G interaction, with the result that the

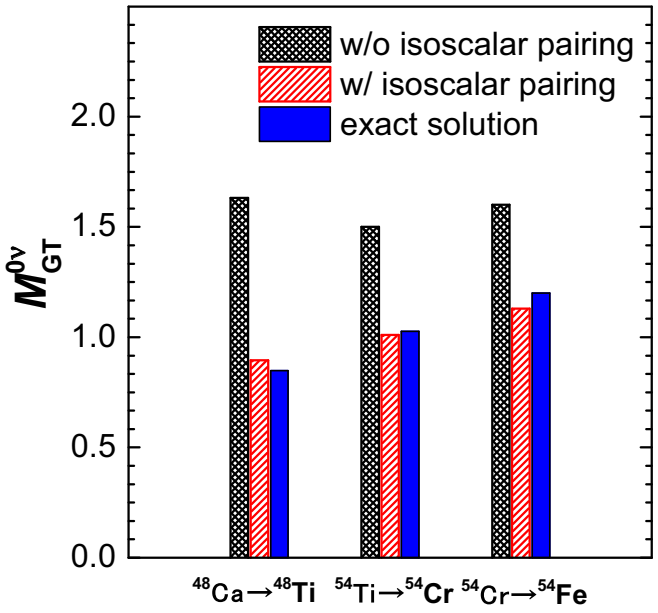

FIG. 1. GCM results for the Gamow-Teller part of $0\nu\beta\beta$ matrix elements of ^{48}Ca, ^{54}Ti, and ^{54}Cr, compared with the results of exact diagonalization.

matrix element decreases, coming quite close to the exact one. The sensitivity to isoscalar pairing, pointed out long ago for the QRPA in Refs. [28] and [29] and more recently for the GCM and shell model in Refs. [14] and [16], shows that the neutron-proton mixing in our HFB states is essential. The good agreement with exact diagonalization suggests that once it is included, we are not omitting anything of importance.

We turn now to one of the nuclei in which we are really interested: ^{76}Ge, used or to be used in many $\beta\beta$ experiments [30–33]. Shell model calculations of the $0\nu\beta\beta$ decay of this nucleus [5, 6, 34, 35] have usually been set in the so-called $f5pg9$ space, comprising the $0f_{5/2}$, $1p_{3/2}$, $1p_{1/2}$, and $0g_{9/2}$ orbits, and have employed either the JUN45 [36] or GCN2850 [37] Hamiltonian. The $f5pg9$ model space is not a complete major shell; it includes levels from two different major shells and is missing, in particular, the spin-orbit partners of the $0f_{5/2}$ and $0g_{9/2}$ orbits. We discuss the effects of including these and other orbits later.

As we already mentioned, both theory [38, 39] and experiment [18, 40] indicate triaxial deformation in low-lying states of even-even Ge and Se isotopes near $A = 76$. Our calculations predict it as well. Figure 2 displays the ^{76}Ge and ^{76}Se quantum-number-projected potential-energy surfaces (PES's), at isoscalar-pairing amplitude $\phi = 0$, produced by the GCM with the GCN2850 interaction. The minimum is at $\beta_2 = 0.23, \gamma = 24°$ in ^{76}Ge, a result that agrees well with those of EDF-based GCM calculations [38], and at at $\beta_2 = 0.28, \gamma = 45°$ in ^{76}Se. In addition to this "static" triaxial deformation (the deformation that would obtain in a pure mean-field calculation), dynamical triaxial deformation, produced by fluc-

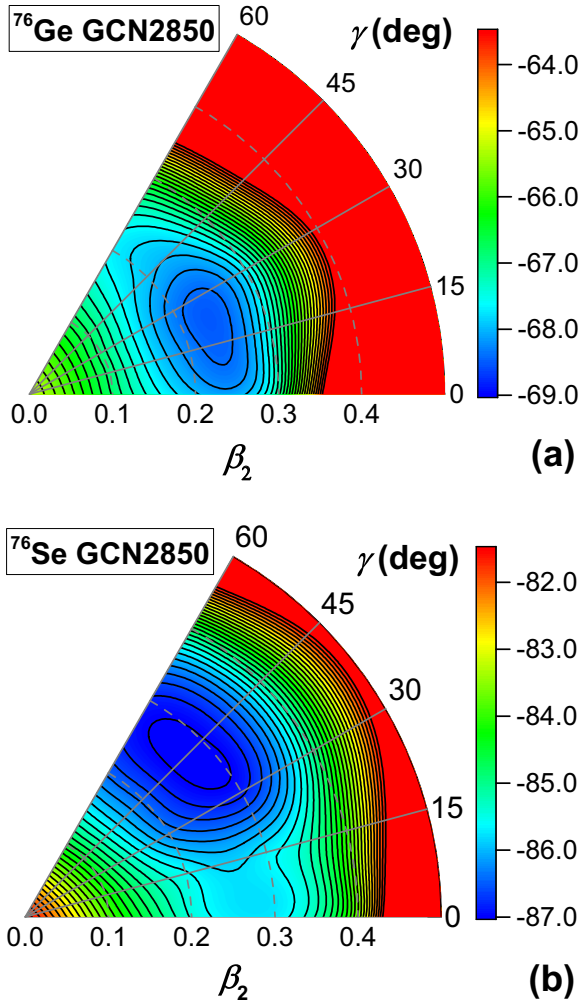

FIG. 2. Projected potential-energy surfaces produced by the GCN2850 interaction, with the isoscalar pairing amplitude $\phi = 0$, in the (β, γ) plane for ^{76}Ge (a) and ^{76}Se (b).

tuations around the dominant mean field, arise from the γ-soft PES's in both isotopes. The GCM, which mixes states with a range of γ values, incorporates these dynamical effects.

Our complete calculations include as generator coordinates both deformation parameters q_1 and q_2 (or equivalently β and γ) as well as one of the proton-neutron-pairing parameters q_3 and q_4. We can assess the effects of triaxial shape fluctuations by including or excluding triaxially deformed configurations from the set of GCM basis states. Including them has clear effects on spectroscopy. Fig 3 shows the spectra of low-lying 0^+ and 2^+ states in the two important $A = 76$ isotopes with GCN2850; triaxial shapes, though they have a relatively small effect on the first excited 0^+ state, lower the second such state significantly in both nuclei, and in ^{76}Se by over an MeV. The values for the strength $B(E2; 0^+ \rightarrow 2^+)$ are affected in a similar way. With triaxial deformation (and with the usual effective charges $e_p^{\rm eff} = 1.5e$ and $e_n^{\rm eff} = 0.5e$) the values in e^2b^2 are 0.172 in ^{76}Ge (vs. the exact-diagonalization value of 0.158) and 0.275 in ^{76}Se (vs. the exact value of 0.209). Without triaxial deformation the numbers are smaller: 0.154 in ^{76}Ge, and 0.268 in ^{76}Se.

	GCN2850	JUN45
Axial GCM	2.71	3.42
Triaxial GCM	2.33	2.94
Exact	2.81 [6]	3.37 [35]

TABLE I. The matrix elements $M^{0\nu}$ produced in the GCM by GCN2850 and JUN45 for the decay of ^{76}Ge, with and with out triaxial deformation as a generator coordinate, and by those same interactions with exact diagonalization.

Triaxial deformation has a non-negligible effect on the $0\nu\beta\beta$ matrix element as well. As Table I shows, our full GCM calculation gives values for the matrix elements $M^{0\nu}$ that are about 15% smaller than the results obtained without triaxially deformed configurations. The full matrix elements, though slightly suppressed, are in good agreement with those of exact diagonalization (in this calculation only, we neglected the very small matrix element $M_T^{0\nu}$). The GCM approach with neutron-proton pairing indeed captures most of correlations around the Fermi surface that are important for $0\nu\beta\beta$ decay. The small discrepancy may be due to fluctuations in like-particle pairing, which we do not treat here but which, according to the EDF-based work of Ref. [12], increase $0\nu\beta\beta$ matrix elements slightly. We could include those fluctuations, but at the cost of a considerable increase in computing time.

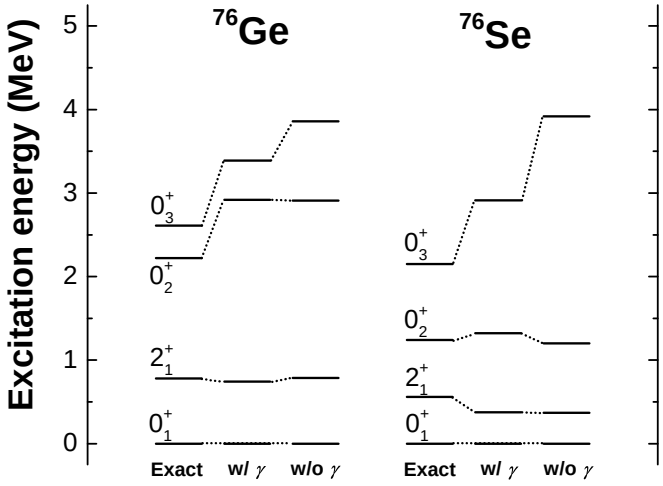

FIG. 3. Low-lying excitation spectra of ^{76}Ge and ^{76}Se produced in one shell by the GCM with the GCN2850 interaction, with and without triaxial deformation (labeled by the parameter γ). The results from the exact diagonalization of the shell-model Hamiltonian appear for comparison [41].

IV. RESULTS IN TWO SHELLS

The promise of the Hamiltonian-based GCM is an eventual *ab initio* calculation. Here we take a step in that direction by working in the full $fp-sdg$ two shell space. The number of states for $A=76$ nuclei in this space is still too large for exact diagonalization.

Before considering Ge and Se, we make one more test, for ^{48}Ca, the one experimental candidate in which an exact two-shell calculation is almost possible at present. Ref. [4] uses the SDPFMU-DB interaction, with the omission of some cross-shell excitations, to compute the $0\nu\beta\beta$ matrix element nearly exactly. Our GCM result, 1.082, is close to 1.073, the result of Ref. [4], and suggests in addition that the cross-shell excitations neglected in that paper really are unimportant. With some confidence in the performance of the GCM in two shells, we turn to the decay of ^{76}Ge.

The first issue we must grapple in this mid-shell nucleus is what to use for the valence-space Hamiltonian. Ref. [14] used a multi-separable collective Hamiltonian that we wish to improve on here. The size of the two-shell space, however, makes the usual procedure, in which shell-model Hamiltonians are tuned to data, difficult to follow; furthermore, there are no well-tested Hamiltonians for this space on the market. The first step in the usual approach is to produce an initial valence-space Hamiltonian, traditionally in many-body perturbation theory. Deficiencies in the many-body method are then remedied by tuning single-particle energies and interaction matrix elements to experimental data. Here we must settle for adjusting only single-particle energies. The tuning of interaction matrix elements requires repeated calculations that are simply too time consuming.

Although nonperturbative methods such as the in-medium similarity renormalization group can produce shell-model Hamiltonians [42, 43], they have not been tested systematically for valence spaces larger than one major harmonic-oscillator shell. We therefore use the Extended Krenciglowa-Kuo (EKK) variant [17] of many-body perturbation theory, suitable for non-degenerate valence spaces, to construct an effective Hamiltonian from a third-order Q-box in the $pf-sdg$ shell. (The original Krenciglowa-Kuo method was first presented in Ref. [44]). We begin from the 1.8/2.0 two- plus three-nucleon (3N) interaction of Refs. [45, 46]; the interaction reproduces ground-state energies across the light- and medium-mass regions of the nuclear chart [47]. With $\hbar\omega=10$ MeV, a space of 13 major shells for intermediate-state sums is enough to ensure convergence.

The monopole components of our valence-space Hamiltonian are particularly sensitive to the initial three-nucleon interaction [48], which one generally reduces to effective zero-, one- and two-body parts via normal ordering with respect to some independent-particle reference state [49]. For shell model calculations, the usual reference state is the inert core, containing all orbitals below the valence space. As discussed in Refs. [50, 51],

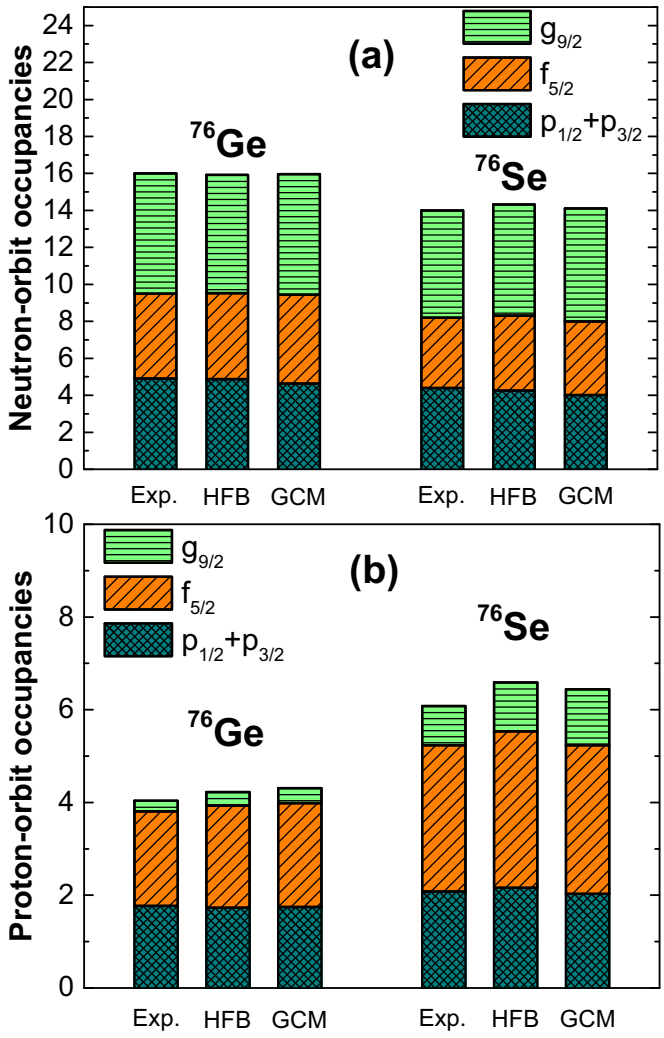

FIG. 4. The occupancies of valence neutron and proton orbits produced by the interaction $pfsdg$ (see text) for ^{76}Ge (a) and ^{76}Se (b), following the adjustment of the single-particle energies for levels in the lower shell. The measured occupancies are from Refs. [52, 53].

however, this choice completely omits three-nucleon interactions among the valence particles themselves, and if the target nucleus (here ^{76}Ge or ^{76}Se) is far from the core, the neglected effects become sizable. Since we can choose to normal-order with respect to any reference we want, it makes sense to include more orbitals, so that we better capture the bulk effects of three-nucleon interactions among valence particles. Thus, we take the reference state to be the (fictional) inert core corresponding to ^{56}Ni. While this nucleus is still some distance in proton and neutron number from the $A=76$ nuclei, we expect it to make a better reference than than the ^{40}Ca core. We call the resulting valence-space interaction $pfsdg$ and use it exclusively in the following.

Perhaps because of the non-ideal reference state, the single-particle energies that emerge from the perturbative procedure are poor. The proton sub-shell gap at

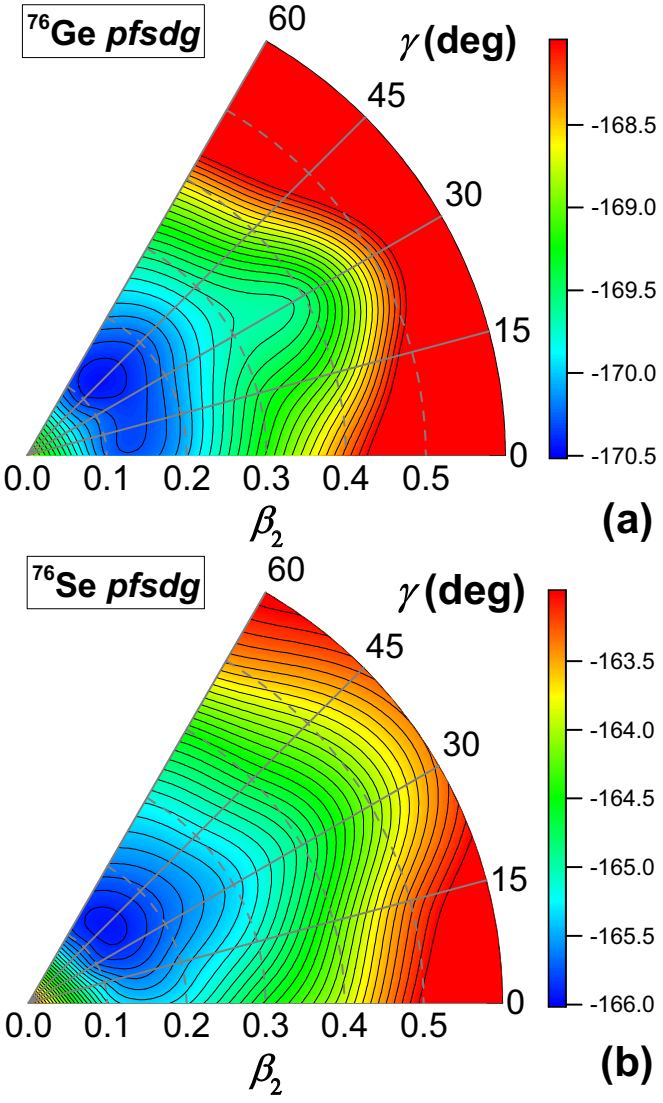

FIG. 5. Potential-energy surfaces for ^{76}Ge (a) and ^{76}Se (b) with the Hamiltonian $pfsdg$.

$Z = 34$ is too large, causing the proton pairing mean field to disappear no matter what the deformation and leading to occupation numbers that differ significantly from measured values. To remedy the problem, we adjust the single-particle energies of the orbits in the lower shell to reproduce those values, while leaving the two-body part of the Hamiltonian untouched. Figure 4 shows the occupation numbers after adjustment, for both the projected HFB state with the minimum energy (which we used to make the adjustments) and in the final GCM states. Though the occupations change a little when the HFB states are mixed in the GCM, they remain close to the experimental values [52, 53].

Figure 5 shows the resulting potential-energy surfaces. The minimum occurs at smaller deformation than in the one-shell example so that, as the calculated spectra in Fig. 6 show, the energy of the first 2^+ state rises noticeably. This worsens the agreement with experiment

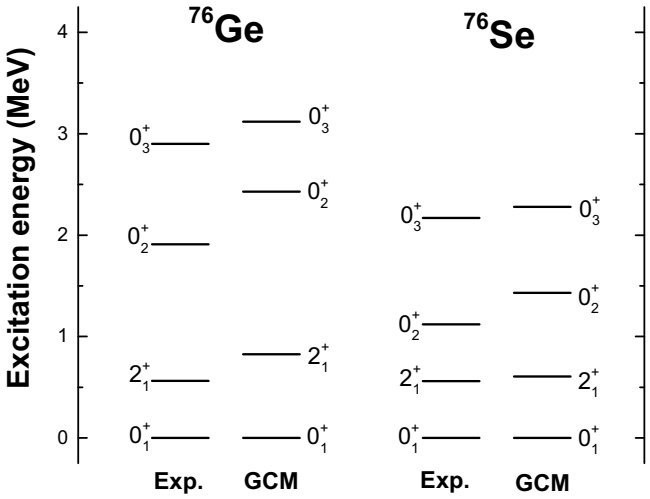

FIG. 6. Calculated low-lying excitation spectra of ^{76}Ge and ^{76}Se produced by the Hamiltonian $pfsdg$ alongside experimental data [54].

slightly in ^{76}Ge, but improves it in ^{76}Se [54]. The excited 0^+ states are also generally better reproduced in the two-shell calculation.

The $B(E2)$ values calculated in two shells are not better than those from one shell, however. With the same effective charges as before, we find noticeably smaller values: 0.126 in ^{76}Ge and 0.221 in ^{76}Se. The corresponding experimental values are larger, 0.274 and 0.432 [54]. Evidently, the $E2$ operator must be renormalized more in two shells than in one, a result that is consistent with the smaller deformation in the two-shell calculation but is nevertheless a little surprising.

We turn finally to the $0\nu\beta\beta$ matrix elements, which appear in Table II. The total matrix element, once triaxial deformation is included, is only slightly larger than that from GCN2850 in a single shell (the second entry in the first column of Table I).

Though our interaction is clearly not perfect, the result suggests that enlarging the space further may not dramatically change the matrix element, though gradual but continual changes with the addition of successive shells cannot be ruled out. It also shows the importance of including triaxial shapes in larger spaces.

Figure 7 summarizes our $\beta\beta$ results. For the decay of

	axial	triaxial
$M^{0\nu}_{\rm GT}$	3.25	2.01
$-\frac{g_V^2}{g_A^2} M^{0\nu}_{\rm F}$	0.43	0.35
$M^{0\nu}_{\rm T}$	−0.03	−0.02
Total $M^{0\nu}$	3.65	2.34

TABLE II. GCM results for thte Gamow-Teller ($M^{0\nu}_{\rm GT}$), Fermi ($M^{0\nu}_{\rm F}$), and tensor ($M^{0\nu}_{\rm T}$) $0\nu\beta\beta$ matrix elements for the decay of ^{76}Ge in two shells, without and with triaxial deformation.

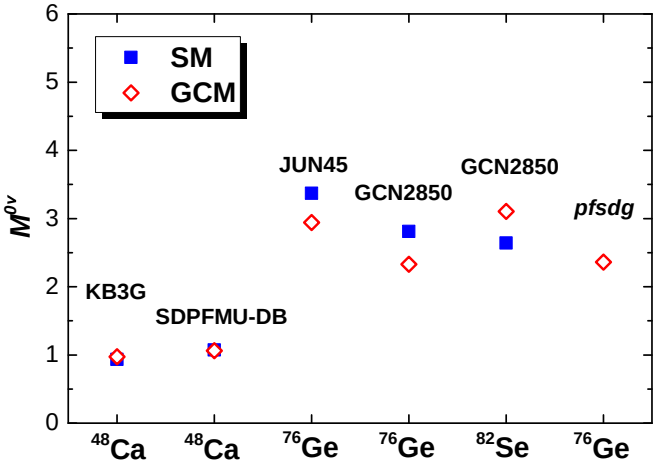

FIG. 7. GCM matrix elements $M^{0\nu}$ compared with those of the shell-model (SM), with either the JUN45 [35], CN2850 [6] KB3G [16], or SDPFMU-DB [4] interactions. The term $pfsdg$ denotes the two-shell interaction used here for $A \approx 80$ nuclei.

^{48}Ca, as noted, we reproduce the exact shell model results nearly perfectly in both one and two shells. For the decay of ^{76}Ge (and ^{82}Se) in a single shell, the GCM reproduces the exact result well enough, with two different effective interactions. And in two shells, with a brand new effective interaction, it obtains a result that is only slightly different from the GCN2850 result in one shell.

An important caveat, in addition to those already mentioned: We really ought to be using an effective $0\nu\beta\beta$ operator to accompany our effective interaction, as in Refs. [55] and [56]. Those papers lead us to suspect a change of 20% or less from an effective decay operator in two shells. In any event, because we made significant phenomenological adjustments to the single-particle energies in the prototype calculation here, we cannot systematically construct the decay operator that should accompany the effective interaction.

V. SUMMARY

The perfect many-body method will include all possible correlations in an infinitely-large space. One step on the way to that ideal is to enlarge the single-particle space for the shell-model, a method that includes all correlations within that space. Here we have approximately diagonalized a shell-model Hamiltonian and computed $0\nu\beta\beta$ transition matrix elements for the decay of ^{76}Ge and ^{82}Se in two major shells, a space well beyond what is typically used. Tests in a single shell, and in two shells for the light pf-shell isotope ^{48}Ca, show that the our approximation method includes the most important correlations. Our first-of-its-kind two-shell calculation in ^{76}Ge suggests a small effect from the extra single-particle orbitals and represents a significant step on the road to accurate $\beta\beta$ matrix elements.

There are at least two ways forward from here. We should use a better effective Hamiltonian, either by normal-ordering with respect to an ensemble reference [51] that better includes bulk effects of three-nucleon forces far from closed shells, or by careful tuning of the interaction. The second option, besides being very difficult, would make it impossible to develop a consistent effective operator, but the first should be pursued. One can also use our GCM wave functions as a starting point for refinement by the "multi-reference" version of the In-Medium Similarity Renormalization Group. Work in that direction is in progress.

VI. ACKNOWLEDGMENTS

We would like to thank J. Menéndez for providing us the unpublished effective interaction GCN2850, J. Simonis for providing matrix elements of normal-ordered three-nucleon interactions, and N. Hinohara, M. Horoi, J. Menéndez, T. R. Rodríguez, and J. M. Yao for helpful discussions. This work has been supported by U.S. Department of Energy grants DE-FG0297ER41019, DE-SC0008641, and DE-SC0004142, by by the National Research Council of Canada, and by NSERC. We used allocations of computing resources at the U.S. National Energy Research Scientific Computing Center (NERSC) and the Jülich Supercomputing Center (JURECA) to carry out computations. Finally, we thank the Institute for Nuclear Theory at the University of Washington for its hospitality and the Department of Energy for partial support during the completion of this work.

[1] F. T. Avignone III, S. R. Elliott, and J. Engel, Rev. Mod. Phys. **80**, 481 (2008).
[2] J. Engel and J. Menéndez, Rept. Prog. Phys. **80**, 046301 (2017), arXiv:1610.06548 [nucl-th].
[3] P. Vogel, J. Phys. G: Nucl. Part. Phys. **39**, 124002 (2012).
[4] Y. Iwata, N. Shimizu, T. Otsuka, Y. Utsuno, J. Menéndez, M. Honma, and T. Abe, Phys. Rev. Lett. **116**, 112502 (2016).
[5] R. A. Sen'kov and M. Horoi, Phys. Rev. C **93**, 044334 (2016).
[6] J. Menéndez, A. Poves, E. Caurier, and F. Nowacki, Nucl. Phys. A **818**, 139 (2009).
[7] J. Barea, J. Kotila, and F. Iachello, Phys. Rev. C **91**, 034304 (2015).
[8] M. T. Mustonen and J. Engel, Phys. Rev. C **87**, 064302 (2013).
[9] F. Šimkovic, V. Rodin, A. Faessler, and P. Vogel, Phys. Rev. C **87**, 045501 (2013).
[10] J. Hyvärinen and J. Suhonen, Phys. Rev. C **91**, 024613 (2015).

[11] T. R. Rodríguez and G. Martínez-Pinedo, Phys. Rev. Lett. **105**, 252503 (2010).
[12] N. L. Vaquero, T. R. Rodríguez, and J. L. Egido, Phys. Rev. Lett. **111**, 142501 (2013).
[13] J. M. Yao, L. S. Song, K. Hagino, P. Ring, and J. Meng, Phys. Rev. C **91**, 024316 (2015).
[14] N. Hinohara and J. Engel, Phys. Rev. C **90**, 031301 (2014).
[15] J. Menéndez, T. R. Rodríguez, G. Martínez-Pinedo, and A. Poves, Phys. Rev. C **90**, 024311 (2014).
[16] J. Menéndez, N. Hinohara, J. Engel, G. Martínez-Pinedo, and T. R. Rodríguez, Phys. Rev. C **93**, 014305 (2016).
[17] N. Tsunoda, K. Takayanagi, M. Hjorth-Jensen, and T. Otsuka, Phys. Rev. C **89**, 024313 (2014).
[18] Y. Toh, C. J. Chiara, E. A. McCutchan, W. B. Walters, R. V. F. Janssens, M. P. Carpenter, S. Zhu, R. Broda, B. Fornal, B. P. Kay, F. G. Kondev, W. Królas, T. Lauritsen, C. J. Lister, T. Pawłat, D. Seweryniak, I. Stefanescu, N. J. Stone, J. Wrzesiński, K. Higashiyama, and N. Yoshinaga, Phys. Rev. C **87**, 041304 (2013).
[19] G. Pantis, F. Šimkovic, J. D. Vergados, and A. Faessler, Phys. Rev. C **53**, 695 (1996).
[20] F. Šimkovic, A. Faessler, V. Rodin, P. Vogel, and J. Engel, Phys. Rev. C **77**, 045503 (2008).
[21] F. Šimkovic, A. Faessler, H. Müther, V. Rodin, and M. Stauf, Phys. Rev. C **79**, 055501 (2009).
[22] A. L. Goodman, *Advances in Nuclear Physics*, edited by J. V. Negele and E. Vogt, Vol. 11 (Plenum Press, New York, 1979) p. 263.
[23] P. Ring and P. Schuck, *The Nuclear Many-Body Problem* (Springer-Verlag, New York, Heidelberg, Berlin, 1980).
[24] T. R. Rodríguez and J. L. Egido, Phys. Rev. C **81**, 064323 (2010).
[25] J. M. Yao, J. Meng, P. Ring, and D. Vretenar, Phys. Rev. C **81**, 044311 (2010).
[26] A. Poves, J. Sánchez-Solano, E. Caurier, and F. Nowacki, Nucl. Phys. A **694**, 157 (2001).
[27] E. Caurier, G. Martínez-Pinedo, F. Nowacki, A. Poves, and A. P. Zuker, Rev. Mod. Phys. **77**, 427 (2005).
[28] P. Vogel and M. R. Zirnbauer, Phys. Rev. Lett. **57**, 3148 (1986).
[29] J. Engel, P. Vogel, and M. R. Zirnbauer, Phys. Rev. C **37**, 731 (1988).
[30] H. Klapdor-Kleingrothaus *et al.*, Eur. Phys. J. A **12**, 147 (2001).
[31] C. E. Aalseth, F. T. Avignone, R. L. Brodzinski, S. Cebrian, E. Garcia, D. Gonzalez, W. K. Hensley, I. G. Irastorza, I. V. Kirpichnikov, A. A. Klimenko, H. S. Miley, A. Morales, J. Morales, A. Ortiz de Solorzano, S. B. Osetrov, V. S. Pogosov, J. Puimedon, J. H. Reeves, M. L. Sarsa, A. A. Smolnikov, A. S. Starostin, A. G. Tamanyan, A. A. Vasenko, S. I. Vasiliev, and J. A. Villar (IGEX Collaboration), Phys. Rev. D **65**, 092007 (2002).
[32] M. Agostini *et al.* (GERDA Collaboration), Phys. Rev. Lett. **111**, 122503 (2013).
[33] N. Abgrall *et al.* (Majorana Collaboration), Adv. High Energy Phys. **2014**, 365432 (2014).
[34] E. Caurier, J. Menéndez, F. Nowacki, and A. Poves, Phys. Rev. Lett. **100**, 052503 (2008).
[35] R. A. Sen'kov and M. Horoi, Phys. Rev. C **90**, 051301 (2014).
[36] M. Honma, T. Otsuka, T. Mizusaki, and M. Hjorth-Jensen, Phys. Rev. C **80**, 064323 (2009).
[37] A. Gniady, E. Caurier, and F. Nowacki, Unpublished.
[38] L. Guo, J. A. Maruhn, and P.-G. Reinhard, Phys. Rev. C **76**, 034317 (2007).
[39] S. F. Shen, S. J. Zheng, F. R. Xu, and R. Wyss, Phys. Rev. C **84**, 044315 (2011).
[40] W.-T. Chou, D. S. Brenner, R. F. Casten, and R. L. Gill, Phys. Rev. C **47**, 157 (1993).
[41] J. Menéndez, (2017), unpublished.
[42] K. Tsukiyama, S. K. Bogner, and A. Schwenk, Phys. Rev. C **85**, 061304(R) (2012).
[43] S. K. Bogner, H. Hergert, J. D. Holt, A. Schwenk, S. Binder, A. Calci, J. Langhammer, and R. Roth, Phys. Rev. Lett. **113**, 142501 (2014).
[44] E. Krenciglowa and T. Kuo, Nuclear Physics A **235**, 171 (1974).
[45] K. Hebeler, S. K. Bogner, R. J. Furnstahl, A. Nogga, and A. Schwenk, Phys. Rev. C **83**, 031301 (2011).
[46] J. Simonis, K. Hebeler, J. D. Holt, J. Menéndez, and A. Schwenk, Phys. Rev. C **93**, 011302 (2016).
[47] J. Simonis, S. R. Stroberg, K. Hebeler, J. D. Holt, and A. Schwenk, Phys. Rev. C **96**, 014303 (2017).
[48] T. Otsuka, T. Suzuki, J. D. Holt, A. Schwenk, and Y. Akaishi, Phys. Rev. Lett **105**, 032501 (2010).
[49] G. Hagen, T. Papenbrock, D. J. Dean, A. Schwenk, A. Nogga, *et al.*, Phys. Rev. C **76**, 034302 (2007).
[50] S. R. Stroberg, H. Hergert, J. D. Holt, S. K. Bogner, and A. Schwenk, Phys. Rev. C **93**, 051301 (2016).
[51] S. R. Stroberg, A. Calci, H. Hergert, J. D. Holt, S. K. Bogner, R. Roth, and A. Schwenk, Phys. Rev. Lett. **118**, 032502 (2017).
[52] J. P. Schiffer, S. J. Freeman, J. A. Clark, C. Deibel, C. R. Fitzpatrick, S. Gros, A. Heinz, D. Hirata, C. L. Jiang, B. P. Kay, A. Parikh, P. D. Parker, K. E. Rehm, A. C. C. Villari, V. Werner, and C. Wrede, Phys. Rev. Lett. **100**, 112501 (2008).
[53] B. P. Kay, J. P. Schiffer, S. J. Freeman, T. Adachi, J. A. Clark, C. M. Deibel, H. Fujita, Y. Fujita, P. Grabmayr, K. Hatanaka, D. Ishikawa, H. Matsubara, Y. Meada, H. Okamura, K. E. Rehm, Y. Sakemi, Y. Shimizu, H. Shimoda, K. Suda, Y. Tameshige, A. Tamii, and C. Wrede, Phys. Rev. C **79**, 021301 (2009).
[54] NuDAT 2.6, http://www.nndc.bnl.gov/nudat2/.
[55] J. D. Holt and J. Engel, Phys. Rev. C **87**, 064315 (2013).
[56] J. Engel and G. Hagen, Phys. Rev. C **79**, 064317 (2009).